



Universiteit
Leiden
The Netherlands

Liposomes as delivery system for allergen-specific immunotherapy

Leboux, R.J.T.

Citation

Leboux, R. J. T. (2021, November 16). *Liposomes as delivery system for allergen-specific immunotherapy*. Retrieved from <https://hdl.handle.net/1887/3240101>

Version: Publisher's Version

License: [Licence agreement concerning inclusion of doctoral thesis in the Institutional Repository of the University of Leiden](#)

Downloaded from: <https://hdl.handle.net/1887/3240101>

Note: To cite this publication please use the final published version (if applicable).

Chapter 5

High-affinity antigen association to cationic liposomes via coiled coil-forming peptides induces a strong antigen-specific CD4+ T-cell response

R.J.T. Leboux¹, N. Benne^{1*}, W.L. van Os², J. Bussmann¹, A. Kros², W. Jiskoot¹, B.A. Slütter^{1#}

¹ Division of BioTherapeutics, Leiden Academic Centre for Drug Research, Leiden University, Leiden, the Netherlands

² Div. of Supramolecular & Biomaterials Chemistry, Leiden Institute of Chemistry, Leiden University, Leiden, the Netherlands

* Current address: Dep. Infectious Diseases and Immunology, Veterinary Science, Utrecht University, Utrecht, the Netherlands

Correspondence: b.a.slutter@lacdr.leidenuniv.nl

Abstract

Liposomes are widely investigated as vaccine delivery systems, but antigen loading efficiency can be low. Moreover, adsorbed antigen may rapidly desorb under physiological conditions. Encapsulation of antigens overcomes the latter problem but results in significant antigen loss during preparation and purification of the liposomes. Here, we propose an alternative attachment method, based on a complementary heterodimeric coiled coil peptide pair pepK and pepE.

PepK was conjugated to cholesterol (yielding CPK) and pepE was covalently linked to model antigen OVA323 (yielding pepE-OVA323). CPK was incorporated in the lipid bilayer of cationic liposomes (180 nm in size). Antigen was associated more efficiently to functionalized liposomes (Kd 166 nM) than to cationic liposomes (Kd not detectable). *In vivo* co-localization of antigen and liposomes was strongly increased upon CPK-functionalization (35% → 80%). CPK-functionalized liposomes induced 5-fold stronger CD4⁺ T-cell proliferation than non-functionalized liposomes *in vitro*. Both formulations were able to induce strong CD4⁺ T-cell expansion in mice, but more IFN- γ and IL-10 production was observed after immunization with functionalized liposomes.

In conclusion, antigen association via coiled coil peptide pair increased co-localization of antigen and liposomes, increased CD4⁺ T-cell proliferation *in vitro* and induced a stronger CD4⁺ T-cell response *in vivo*.

Introduction

The latest generation of vaccines moves away from whole pathogens and instead uses pathogen-derived proteins or peptides (i.e., subunits) as antigen. Subunit based vaccines are safer than whole pathogen-based vaccines but require adjuvants because these antigens alone are poorly immunogenic. Liposomes, vesicles composed of a phospholipid bilayer, are a widely investigated adjuvant because of their versatility and proven success [1-4]. The lipid composition directs the physico-chemical properties of the liposomes, such as size, zeta potential, membrane fluidity and rigidity [1, 3]. These properties greatly influence their behavior upon injection and the immune response they may induce [3, 5-8]. Cationic liposomes have been used extensively as vaccine adjuvants. They are known to induce strong T-cell expansion and pro-inflammatory T helper (Th) 1-skewed immune response [9-14].

For a maximum adjuvant effect, the adjuvant and antigen need to be taken up by the same antigen presenting cell. This is most efficiently achieved when the antigen and the adjuvant are physically or chemically associated [15, 16]. Antigens can be associated with liposomes in various ways. For instance, hydrophilic molecules can be encapsulated in the aqueous core, whereas lipophilic molecules can be incorporated in the lipid bilayer. Although encapsulation usually ensures sustained co-localization, the encapsulation of an antigen in liposomes can be a challenging and costly process. Very few examples have shown 100% encapsulation efficiency, which oftentimes means that a large amount (up to 99%) of a valuable antigen is lost during liposome preparation and purification [10, 17-19]. Moreover, the encapsulation process has to be optimized for each new antigen, and might require a change of composition of the liposomes, thereby potentially sacrificing adjuvant potential [19, 20]. A more straightforward method is association of antigens on the outside of the liposome, which could be achieved by simple mixing of the antigen with preformed liposomes. Administration of antigens adsorbed to liposomes, via electrostatic interaction, has been shown to enhance the induced immune response compared to administration of plain antigen [12, 21]. However, the degree of association may vary between antigens and formulations [22-25]. Moreover, after administration of liposomes with electrostatically adsorbed antigen, the antigen may rapidly diffuse away from the liposomes because of competition between the antigen and extracellular biomolecules. Another disadvantage of electrostatic adsorption of antigens is that it requires an opposite charges on the liposome and antigen [26]. This complicates the development of a general vaccine adjuvant that can be used for a diverse range of antigens.

Here we provide an attractive alternative method of antigen association to functionalized liposomes based on designer coiled coil (CC) motifs. In this method,

complementary peptides interact resulting in the formation of noncovalent intermolecular helices [27, 28]. The formation of these helices is based on a complementary peptide pair, peptide E (pepE) and peptide K (pepK), which form a parallel heterodimer CC [27-29]. The pepE-pepK peptide pair has been shown to remain intact under physiological conditions. Moreover, liposomes functionalized with pepK have shown to be able to target cells functionalized with pepE *in vitro* and *in vivo* [30-34]. We investigated the possibility to use this CC forming peptide pair as an attachment platform for association of antigens to liposomes. We hypothesized that the binding affinity of these CC-forming peptides results in a higher association efficiency of the antigen and a more stable association *in vivo* as compared to electrostatic interaction. Here we report that indeed the association of antigen (pepE-OVA323) with pepK-functionalized liposomes remained intact under physiological conditions. Moreover, we show this way of association significantly enhanced the immunogenicity of the antigen, resulting in a stronger CD4⁺ T-cell activation.

Material and Methods

Chemicals

Cholesterol (Chol), 1,2-distearoyl-sn-glycero-3-phosphocoline (DSPC) and 1,2-dioleoyl-3-trimethylammonium-propane (DOTAP) were purchased from Avanti Lipids (AL, USA). OVA323-339 and granulocyte-macrophage colony-stimulating factor (GM-CSF) were supplied by Bio-Connect (Huissen, Netherlands), 1,1'-Diocetadecyl-3,3,3',3'-Tetramethylindodicarbocyanine, 4-Chlorobenzenesulfonate (DiD), phorbol 12-myristate 13-acetate (PMA), ionomycin, Brefeldin A, Penicillin-Streptomycin (PenStrep), GlutaMAX[™] were supplied by Thermo Fisher (Bleiswijk, Netherlands). Iscove's Modified Dulbecco's Medium (IMDM) and Roswell Park Memorial Institute 1640 (RPMI) were supplied by Lonza (Basel, Switzerland). Fetal Calf Serum (FCS) was purchased from PAA Laboratories (Ontario, Canada). Dimethylformamide (DMF), piperidine, acetic anhydride, pyridine, trifluoroacetic acid (TFA) and acetonitrile (ACN) were purchased from Biosolve (Valkenswaard, Netherlands). N,N-diisopropylethylamine (DIPEA), and Ethyl cyanohydroxyiminoacetate (Oxyma) were obtained from Carl Roth (Karlsruhe, Germany). Dichloromethane (DCM) and diethyl ether were supplied by Honeywell (Landsmeer, Netherlands). Tentagel HL-RAM was obtained from Rapp Polymere (Tübingen, Germany). All amino acids were supplied by NovaBioChem (Darmstadt, Germany). Fmoc-NH-PEG₄-COOH was purchased from Iris Biotech GmbH (Marktredwitz, Germany) All fluorescent antibodies for flow cytometry were purchased from eBioscience (MA, USA) and are displayed in supplementary table 1. CD4 and CD8 T-cell enrichment kit was purchased from Miltenyi (Leiden, Netherlands). All other chemicals were purchased from Sigma Aldrich (Zwijndrecht, Netherlands).

Mouse experiments

C57Bl/6, OT-I and OT-II transgenic mice on a C57Bl/6 background were purchased from Jackson Laboratory (CA, USA), bred in-house under standard laboratory conditions, and provided with food and water *ad libitum*. All animal work was performed in compliance with the Dutch government guidelines and the Directive 2010/63/EU of the European Parliament. Experiments were approved by the Ethics Committee for Animal Experiments of Leiden University.

Peptide synthesis

Peptides were synthesized on a microwave-assisted, automated peptide synthesizer (Liberty Blue). An overview of all the synthesized compounds can be found in Supplementary table 2. Synthesis was performed at a 0.1 mmol scale on the solid-phase Tentagel HL-RAM resin with a loading of 0.39 mmol/g. Fmoc-deprotection was achieved with 20% piperidine in DMF at 90 °C for 60 s. Amide coupling was achieved using 5 equiv. of Fmoc-protected amino acid with 5 equiv. of DIC as activator and 5 equiv. of Oxyma as the activator base heated at 95 °C for 240 s. Upon completion of synthesis, peptides were acetylated with an excess of acetic anhydride and pyridine in DMF. Cholesterol-coupled pepK (CPK) was synthesized as described elsewhere [35]. In short, resin-bound peptides were PEGylated with 2.5 equiv. of Fmoc-NH-PEG₄-COOH in the presence of 5 equiv. of DIPEA and 2.5 equiv. of HATU for 4 hours at room temperature. Subsequently, the protecting Fmoc was removed with 20% piperidine in DMF and the reactive amine was coupled to 1.05 equiv. amino-cholestene hemisuccinate in the presence of 5 equiv. DIPEA and 2.5 equiv. HATU for 4 hours at room temperature, before cleavage from the resin was performed by using a mixture of TFA:TIPS:water, 95:2.5:2.5. The peptide was precipitated in ice-cold diethyl ether; the precipitate was subsequently collected by centrifugation and dissolved in a water and ACN mixture. The ACN was removed using a rotary evaporator and water was removed by lyophilization, resulting in crude peptide as an off-white powder.

All peptides and conjugates were purified by reversed-phase HPLC (RP-HPLC) on a Kinetic Evo C18 column with a Shimadzu system comprising two LC-8A pumps and an SPD-10AVP UV-Vis detector. Peptides were purified using a gradient of 20-80% B, (where B is ACN containing 1% TFA, and A is water with 1% TFA) over 20 minutes with a flow rate of 12 mL/min. The collected fractions were analyzed on a LC-MS system (Thermo Scientific TSQ quantum access MAX mass detector connected to a Ultimate 3000 liquid chromatography system fitted with a 50 × 4.6 mm Phenomenex Gemini 3 μm C18 column) and those deemed to be pure were pooled. Organic solvent was removed under reduced pressure (150 mbar) before lyophilization to obtain a dry purified peptide powder.

AlexaFluor488-labeled pepE-OVA323 was synthesized starting from pepE-OVA323 with an additional glycine and cysteine at the C-terminus. The peptide

was incubated with 1.1 equiv. AlexaFluor 488 C₅ maleimide (Thermo Fisher, Netherlands) in 100 mM HEPES buffer (pH 7.4) in the dark at room temperature. After 2 hours, free dye was removed by dialysis under constant stirring in a 2k MWCO Slide-A-Lyzer™ (Thermo Fisher, Netherlands) at 4 degrees to Milli-Q (18,2 MOhm/cm) overnight. Finally, the pure peptide was obtained by centrifugation at 1,000 x g for 30 minutes.

Liposome preparation and characterization

Liposomes were prepared by the dehydration-rehydration method as described elsewhere [17]. In brief: 15 μmol total lipids with or without CPK were dissolved in 1:2 methanol:chloroform in the desired ratio (2:1:1 DSPC:DOTAP:cholesterol molar ratio with 1 mol% CPK). In case of fluorescent liposomes, 0.1 mol% of total lipid DiD was added in this step. Subsequently, the organic solvent was evaporated at 150 mbar and 50 °C in a rotary evaporator, yielding a lipid film. This film was hydrated in the presence of glass beads with a 10 mM HEPES, 280 mM sucrose, pH 7.4 (H/S buffer), with antigen in the case of encapsulation, frozen in liquid nitrogen and lyophilized overnight. The resulting lipid cake was rehydrated with Milli-Q to a final volume of 1 mL (resulting in a 15 mM lipid suspension) and homogenized with a LIPEX extruder (Evonik, Canada) by repeated passage over stacked filters of 400 nm and 200 nm (Nuclepore Track-Etch membrane from Whatman, Netherlands).

Hydrodynamic diameter and polydispersity were measured by dynamic light scattering (DLS) using a Zetasizer Nano ZS (Malvern Instruments Ltd., Worcestershire, UK). The zeta potential was measured using laser Doppler electrophoresis on the same machine with a zeta dip cell (Malvern Instruments Ltd.). Each sample was diluted 100-fold in 10 mM HEPES buffer (pH 7.4) before measurement.

Isothermal titration calorimetry

Isothermal titration calorimetry (ITC) was performed with a MicroCal PEAQ-ITC Automated machine (Malvern Instruments Ltd., Worcestershire, UK). Free pepK or liposomes containing CPK (300 μl, 50 μM pepK or CPK in H/S buffer) were used in the receptor compartment. 3 μl of pepE, pepE-OVA323 or pepE-OVA257 (500 μM) was added every 180 seconds.

For data analysis, the first injection was removed from the raw data. Subsequently a One-sided fitting was performed, which was optimized by 100 iterations until the values for binding constant, stoichiometry and dH did not change anymore.

Far-UV circular dichroism spectroscopy

Far-UV circular dichroism (CD) measurements were performed on a Jasco J815 CD spectrometer equipped with a Jasco PTC 123 Peltier temperature controller

in a 1 mm quartz cuvette. Far-UV CD spectra between 190–260 nm were also collected at T = 25°C. The molar ellipticity $[\theta]$ was calculated from the measured ellipticity θ , the path length l in centimeter, the molar monomer concentration cM , and the number of amino acids per peptide N as:

$$[\theta] = \frac{100 \cdot \theta}{l \cdot ((cM1 \cdot N1) + (cM2 \cdot N2))} \quad (\text{Equation 1})$$

as described elsewhere [36].

Association efficiency

To determine the association efficiency of pepE-OVA323 to liposomes, liposomes with and without CPK (800 μg lipids/mL) were incubated with antigen (30 μg /mL) for 30 minutes. Subsequently, unbound antigen was separated from liposomes with a centrifuge membrane concentrator (Vivaspin2, 300.000 MWCO, Sartorius) by spinning down for 10 minutes at 500 x g. The unbound fraction (flow through) was measured by RP-UPLC (Waters ACQUITY UPLC, Waters, MA, USA).

Liposomes with and without CPK (800 μg lipids/mL) were mixed with pepE-OVA257 (30 μg /mL) and dialyzed in a Float-A-Lyzer[®] G2 (Spectrum labs, CA, United States) of 1 mL and MWCO of 100 kD for 5 days against 10 mM HEPES buffer pH 7.4. Remaining antigen in the dialysis membrane was measured by RP-UPLC (Waters ACQUITY UPLC, Waters, MA, USA).

Ex vivo T-cell stimulation

Bone marrow-derived dendritic cells (BMDCs) were prepared as described elsewhere [37]. In short, bone marrow was isolated from murine tibia and femurs of C57BL/6 mice. Bone marrow cells were stimulated for 10 days with 20 ng/mL GM-CSF in complete IMDM (cIMDM, IMDM supplemented with 100 U/mL PenStrep, 2 mM glutaMAX and 8% FCS). After 10 days, the BMDCs (50,000 cells per well) were exposed to the different formulations for 4 hours. Subsequently the BMDCs were washed twice with cIMDM and incubated with either 100,000 CD4⁺ T-cells derived from OT-II mice or 100,000 CD8⁺ T-cells derived from OT-I mice, which were purified according to manufacturer's protocol [38], for 72 hours in complete RPMI (cRPMI, supplemented with 100 U/mL PenStrep, 2 mM glutaMAX, 50 μM β -mercaptoethanol and 10% FCS). After 72 hours, the cell suspension was harvested and prepared for flow cytometry.

Flow cytometry measurements and analysis

For flow cytometry measurements, the cell suspension was washed with FACS buffer (PBS with 1% FCS and 2 mM EDTA). Subsequently, the suspension was stained for 30 minutes in the dark at 4 °C with FACS buffer containing fluorescent antibodies against the surface markers of interest (an overview of the used antibodies is found in Supplementary table 1). After the staining, the

cells were washed with PBS and measured in the flow cytometer (CytoFLEX S, BeckmanCoulter, CA, US). For intracellular markers, the cells were subsequently fixed and stained according to manufacturer's protocol with the Transcription Factor Staining Buffer Set (eBioscience, catalogue number 00-5523-00) for transcription factors, or the Intracellular Fixation & Permeabilization Buffer Set (eBioscience, catalogue number 88-8824-00). Before measurement, the cells were resuspended in PBS. All flow cytometry data were analyzed using FlowJo vX.

Peptide uptake in BMDCs

BMDCs were prepared as described above and 50,000 BMDCs per well were plated in a flat bottomed 96 wells plate. Subsequently, different liposome formulations containing DiD (ex/em wavelength: 644/665 nm) were added to the culture medium of these BMDCs. After 4 hours, cell medium was refreshed twice to remove any unbound formulation. Subsequently, cells were prepared for flow cytometry.

Biodistribution studies in zebrafish embryos

Zebrafish (*Danio rerio*, strain AB/TL or Tg(kdrl:RFP-CAAX)_{s916} [39]) were maintained and handled according to the guidelines from the Zebrafish Model Organism Database (<http://zfin.org>) and in compliance with the directives of the local animal welfare committee of Leiden University. Fertilization was performed by natural spawning at the beginning of the light period, and eggs were raised at 28.5 °C in egg water (60 g/mL Instant Ocean sea salts). Prior to injection, zebrafish embryos were embedded and anesthetized in 0.4% agarose containing 0.01% tricaine. Liposomal formulations (containing 5 mM lipids and/or 200 µg/ml pepE-OVA323-AF488) were injected with 1 nL volume in the duct of Cuvier. at 2.5 days post fertilization (dpf) as described previously [40]. For each treatment, two independently formulated liposome preparations were imaged using confocal microscopy. Embryos were randomly picked from a dish of 10-20 successfully injected embryos (exclusion criteria were: no backward translocation of erythrocytes after injection and/or damage to the yolk ball).

Confocal z-stacks were captured on a Leica TCS SPE confocal microscope, using a 10× air objective (HCX PL FLUOTAR) or a 40× water-immersion objective (HCX APO L). For whole-embryo views, 3–5 overlapping z-stacks were captured to cover the complete embryo. Laser intensity, gain, and offset settings were identical between stacks and sessions. Images were processed using the Fiji distribution of ImageJ [41, 42]. The greyscale threshold for both liposomal and peptide signal was determined and set identical for an entire experiment. All pixels with intensity above the threshold were set at a maximum value of 255, whereas negative pixels were set at 0. Subsequently, the “3D-multi coloc” plugin

of 3d Image suite was used to determine co-localization [43].

Adoptive transfer and vaccination study

C57Bl/6 mice (10-15 week-old females) were randomized into groups. On day 0, all mice received 500,000 CD4⁺ T-cells, that were purified from sex-matched OT-II transgenic mice with a CD4⁺ T-cell enrichment kit (Miltenyi, Netherlands) according to manufacturer's protocol [38], via the tail vein. On day 1, mice were immunized subcutaneously with a single injection of formulation in a total volume of 200 μ l in H/S buffer. Seven days after immunization, mice were sacrificed and blood, spleen and axillary and brachial lymph nodes (LNs) were removed. Organs were processed and measured by flow cytometry.

Splenocytes (10^6 per well) of each mouse were stimulated in cRPMI for 1 hour with either medium, pepE-OVA323, or PMA and ionomycin, after which brefeldin A was added and the cells were incubated for another 5 hours and subsequently prepared for flow cytometry.

Statistical analysis

Data was processed and analyzed in GraphPad v8 (Prism) for Windows. Statistical analysis was performed with the same program and the method of analysis is indicated in the figure legends.

Results

Peptide and liposome characterization

The MHC-II (I-A^b) restricted epitope of ovalbumin (OVA323-339, ISQAVHAAHAEINEAGR) was synthesized at the C-terminus of pepE resulting in the pepE-OVA323 conjugate. The same was done for the MHC-I (H2-K^b) restricted epitope (OVA257-264, SIINFEKL), resulting in pepE-OVA257. All peptides were of >95% purity according to RP-HPLC (Supplementary figures 1-4). Subsequently, positively charged (DOTAP-containing) liposomes were prepared with and without CPK to assess the effect of its incorporation on the physico-chemical properties of liposomes composed of DOTAP, DSPC and cholesterol. The size (179 vs 177 nm for liposomes without and with CPK respectively), polydispersity index (PDI, 0.073 vs 0.071 for liposomes without and with CPK respectively) and zeta potential (between 48 vs 45 mV for liposomes without and with CPK respectively) of liposomes were unaffected by the addition of 1 mol% CPK (Table 1).

Table 1. Overview of the particle size (z-average), polydispersity index (PDI) and zeta potential of non-functionalized liposomes (DOTAP:DSPC:cholesterol) and CPK-functionalized liposomes before and after mixing with pepE-OVA323 or pepE-OVA257. Moreover, the dissociation constant (Kd) as measured by ITC is shown. * = significantly different than the liposomes without antigen. # = beyond detection limit. Values represent average values \pm SD ($n \geq 2$). N.a. = not applicable.

Liposome formulation	Z-average (nm)	PDI	Zeta potential (mV)	Kd (nM)	Association efficiency (%)
Non-functionalized liposomes	179.3 \pm 13.8	0.073 \pm 0.039	48.1 \pm 3.3	n.a.	n.a.
CPK-functionalized liposomes	176.7 \pm 14.4	0.071 \pm 0.047	44.9 \pm 6.2	n.a.	n.a.
Non-functionalized liposomes + pepE-OVA323	188.6 \pm 6.6	0.116 \pm 0.028 *	35.0 \pm 5.2 *	> 10 ⁵ #	78.1 \pm 4.0
CPK-functionalized liposomes + pepE-OVA323	185.8 \pm 4.2	0.080 \pm 0.014	28.6 \pm 7.0 *	166 \pm 68	>95% #
Non-functionalized liposomes + pepE-OVA257	182.5 \pm 2.3	0.092 \pm 0.004	45.0 \pm 2.4	> 10 ⁵ #	1.69 \pm 2.4
CPK-functionalized liposomes + pepE-OVA257	184.6 \pm 2.5	0.089 \pm 0.004	38.8 \pm 1.3 *	392 \pm 264	47.5 \pm 7.1

To confirm the presence of CPK in the functionalized liposomes, and the ability of CPK to interact with pepE-conjugates, we performed far-UV CD spectroscopy and ITC, respectively. Far-UV CD spectra showed minima at 222 and 208 nm in CPK-functionalized liposomes which indicates presence of α -helices. Upon mixing with pepE, the peak at 208 nm and overall signal increased, pointing to interaction and the formation of a CC structure (Supplementary figure 5). ITC was used to determine the binding energy and dissociation constant (Kd) between peptide and liposome. No binding energy was measured in non-functionalized liposomes (Figure 1), whereas the binding energy of pepE and pepE-conjugates titrated into a suspension of CPK-functionalized liposomes decreased slowly during the first 6 injections after which a plateau was reached (Figure 1). Kd values were determined for both pepE-conjugates onto CPK-functionalized liposomes and all were in the order of 10⁻⁷ M, but could not be measured with non-functionalized liposomes. Moreover, antigen was mixed with both formulations and unbound antigen was removed by centrifugal filtration or dialysis to measure association efficiency. We observed an association efficiency of 78% after mixing pepE-OVA323 with non-functionalized liposomes, which substantially increased after mixing with functionalized liposomes (Table 1), where the unbound antigen concentration was below the limit of detection. Thus, CC interaction provided a simple and highly efficient method to associate antigen to liposomes, which appeared stronger than adsorption to non-functionalized liposomes.

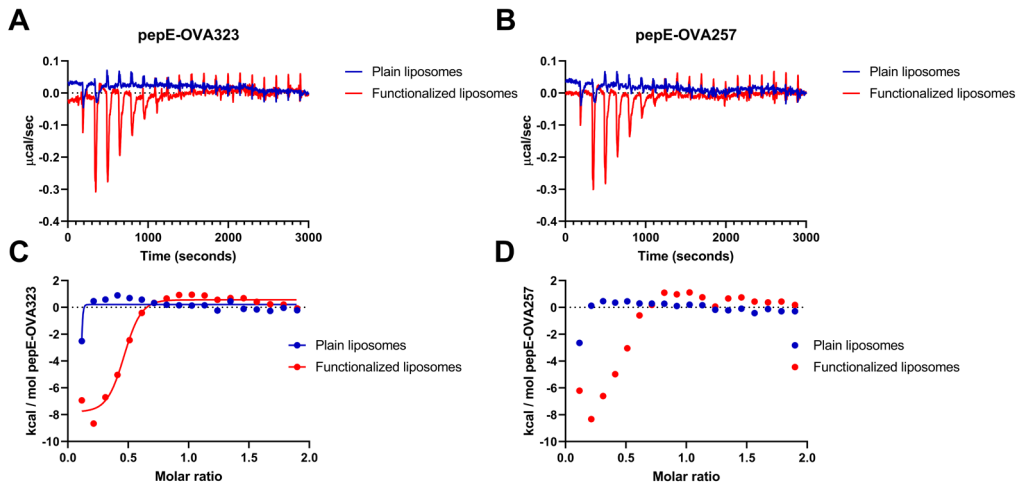


Figure 1. Antigen binding to liposomes. Buffer corrected heat plots of isothermal titration calorimetry measurements in which non-functionalized and functionalized liposomes were titrated with pepE-OVA323 (A) and pepE-OVA257 (B). The calculated energy per mol of pepE-OVA323 (C) or pepE-OVA257 (D) was used to derive the dissociation constant K_d (B).

Peptide uptake in BMDCs

We assessed whether the increased affinity provided by CC-mediated association would result in an increased antigen and liposome uptake by BMDCs. Fluorescently labeled pepE-OVA323 and the DiD-labeled fluorescent liposomes were used to facilitate cell uptake studies using flow cytometry. The incorporation of a small amount of fluorescent dye resulted in a slightly smaller size (160 vs 180 nm) of the liposomes (Supplementary Figure 6), but . BMDCs were incubated for 4 hours with fluorescent formulations containing pepE-OVA323. Over 90% of all BMDCs had taken up liposomes, irrespective of CPK-functionalization or presence of antigen (Figure 2). However, dendritic cells had taken up antigen in presence of CPK-functionalized liposomes. Uptake of peptides in the absence of liposomes was limited (39%). Association with non-functionalized liposomes increased the uptake from 40% to 75%, but was this increased to >99% after association to CPK-functionalized liposomes (Figure 2A). The fluorescent signal in cells (Mean Fluorescence Intensity, MFI) after exposure to pepE-OVA323 was significantly increased with functionalized liposomes (20-fold), compared to a 4-fold increase by association to non-functionalized liposomes (Figure 2B), which indicates more uptake of pepE-OVA323 per cell. These data show that under physiological conditions (including serum), the strong association of antigen to CPK functionalized liposomes via coiled coil formation results in an improved uptake of the antigen.

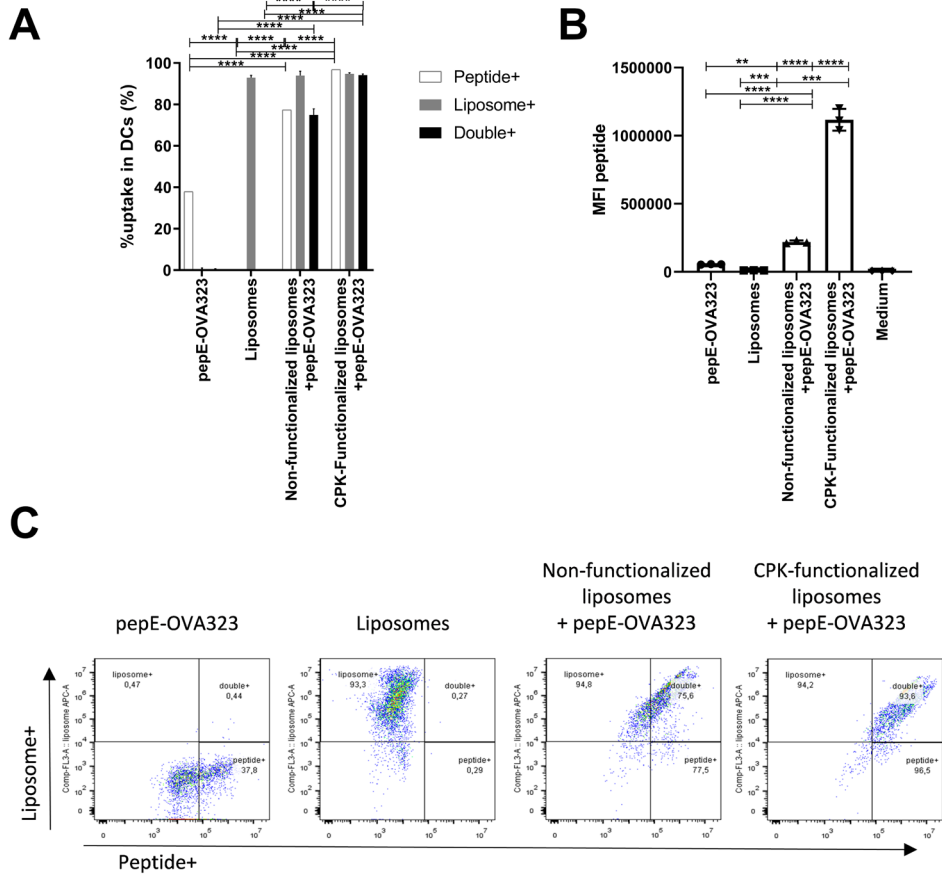


Figure 2. Uptake of pepE-OVA323 and liposomes in MHCII⁺CD11c⁺ BMDCs. BMDCs were incubated in cIMDM for 4 hours with different formulations containing fluorescent liposomes and fluorescent pepE-OVA323. Subsequently, the BMDCs were analyzed by flow cytometry for peptide and liposome uptake. C shows representative FACS plots of BMDC population for each formulation. A Two-way ANOVA with a Tukey's multiple comparison test was performed to determine statistically significant differences in antigen and liposome uptake. MFI was compared with a One-way ANOVA and Tukey's multiple comparison test. ** = $p < 0.01$, *** = $p < 0.001$, **** = $p < 0.0001$.

In vivo distribution in zebrafish embryos

The *in vitro* studies revealed that CPK-functionalized liposomes increased antigen and liposome co-localization compared to non-functionalized liposomes. To evaluate how these *in vitro* findings translate to *in vivo* administration in complex tissue, we investigated the biodistribution of pepE-OVA323 and cationic liposomes after intravenous injection in zebrafish embryos. Free peptide, free liposomes, non-functionalized and CPK-functionalized liposomes incubated with pepE-OVA323 were injected in zebrafish embryos. Confocal fluorescence

microscopy was used to assess the biodistribution of both liposomes and peptides after injection. Co-localization throughout the embryo was observed after injection of functionalized liposomes with pepE-OVA323, and was especially prominent in the caudal vein (Figure 3A, B). In contrast, for cationic liposomes with pepE-OVA323, co-localization was only observed in the caudal aspect of the tail and at the injection site for non-functionalized liposomes with pepE-OVA323 (Figure 3A). Non-functionalized liposomes that were associated with pepE-OVA323 displayed similar distribution to the individual components alone (Supplementary figure 7). This difference of pepE-OVA323 distribution after association with functionalized liposomes and non-functionalized liposomes was more profound when zoomed in on the tail vein (Figure 3B). We observed 75% of the functionalized liposome signal co-localized with pepE-OVA323, in contrast to pepE-OVA323 associated to non-functionalized liposomes (34%) (Figure 3C). In 3D representation, the co-localization can be observed at the subcellular level

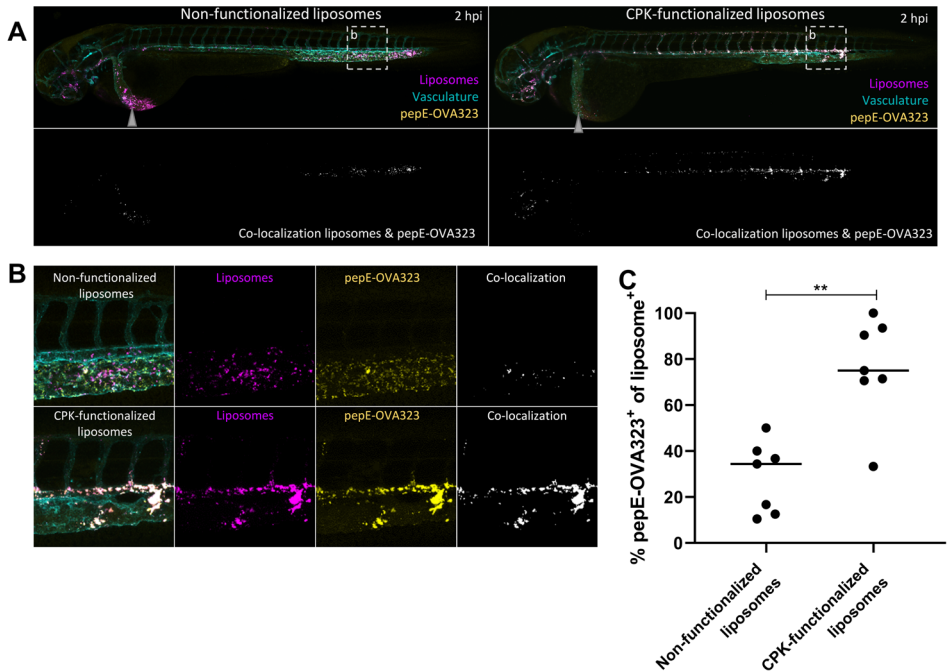


Figure 3. Liposome and antigen distribution in zebrafish embryos. Representative images of zebrafish embryos 2 hours post injection (hpi) of pepE-OVA323 adsorbed to non-functionalized liposomes and CPK-functionalized liposomes. Gray arrows indicate the site of injection. Images were taken by confocal microscopy at 10x magnification (A) and 40x magnification (B), compressed and processed by ImageJ. PepE-OVA323 (yellow), liposomes (magenta) and the vascular system (cyan; *kdr1:mCherry*) of the zebrafish are shown in the upper image; co-localization of pepE-OVA323 and liposomes (i.e., the pixels in which the signals of fluorescence were above the background signal) is white in the lower image of whole fish (A). The percentage of all pixels that had liposome signal which also had pepE-OVA323 signal (C) was compared with a Mann Whitney test, ** = $p < 0.01$.

as well (Supplementary video 1 and 2). Thus, pepE-OVA323 remained strongly associated with functionalized liposomes *in vivo*, but only in part associated with non-functionalized liposomes.

Ex vivo T-cell stimulation and proliferation

Next, we investigated whether the strong association and co-localization of antigen and liposome results in improved immunogenicity. We pulsed BMDCs with plain pepE-OVA323 or pepE-OVA323 adsorbed to liposomes with and without CPK for 4 hours, after which CD4⁺ T-cells derived from OT-II transgenic mice were co-cultured with these BMDCs. We observed that BMDCs pulsed with soluble pepE-OVA323 successfully induced concentration-dependent T-cell proliferation (Figure 4A). Compared to plain peptide, BMDCs pulsed with pepE-OVA323 associated with non-functionalized liposomes resulted in an approximately 5-fold lower EC50. The same antigen associated to CPK-functionalized liposomes, however, showed an 18-fold lower EC50 than soluble peptide.

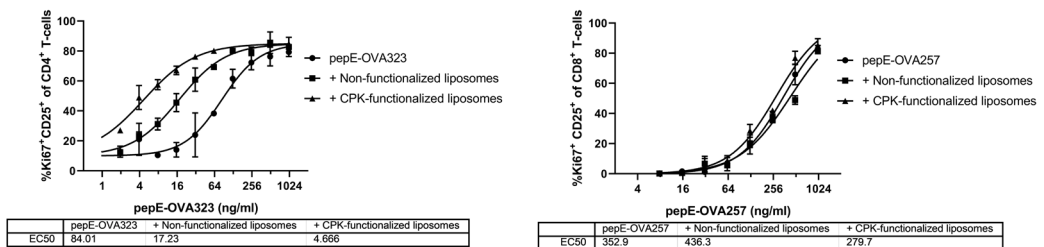


Figure 4. *In vitro* T-cell proliferation. A) CD8⁺ T-cell proliferation induced by BMDCs pulsed with pepE-OVA257 in different formulations. B) CD4⁺ T-cell proliferation induced BMDCs pulsed with pepE-OVA323 in different formulations. EC50 values were calculated based on a non-linear dose-response model fit with variable slope (four parameters) in which top and bottom were shared between all groups. Graph shows average of 3 points for each concentration and is a representative of 3 separate experiments.

A similar experiment was performed with pepE-OVA257, an MHC-I restricted epitope of ovalbumin and CD8⁺ T-cells derived from OT-I transgenic mice. There we also found a concentration-dependent T-cell proliferation profile. Interestingly, in contrast to the CD4⁺ T-cell proliferation, there were no differences in proliferation induced by plain peptide, or antigen associated with either liposome formulation (Figure 4B).

In vivo immune response in mice

As both non-functionalized and CPK-functionalized liposomes increased the CD4⁺ T-cell responses *in vitro*, we vaccinated mice that had received an adoptive transfer of ovalbumin-specific CD4⁺ T-cells derived from OT-II mice to compare

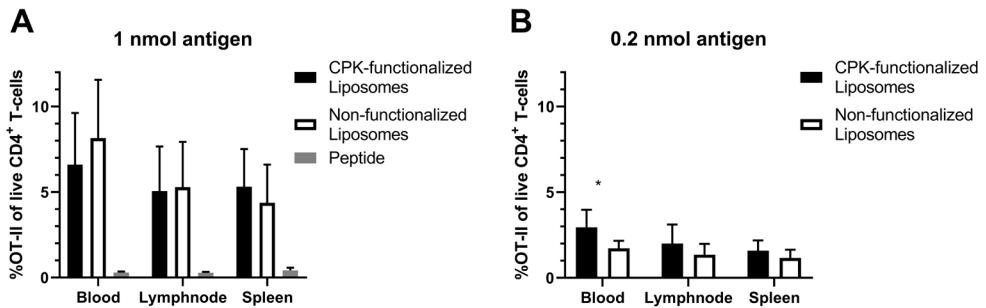


Figure 5. OT-II T-cell expansion after vaccination. OT-II CD4⁺ T-cell expansion *in vivo* induced by vaccination with 1 nmol antigen (A, mean \pm SD, n = 8 for liposomes, n = 4 for peptide) and 0.2 nmol antigen (B, mean \pm SD, n = 7) as measured by flow cytometry. Effect of the formulation in each organ was compared by multiple student's t tests. * = $p < 0.05$

the effect of non-functionalized and CPK-functionalized liposomes on the *in vivo* immunogenicity. One day after the adoptive transfer, mice received pepE-OVA323 in buffer or associated to either non-functionalized or CPK-functionalized liposomes. The expansion of the transferred CD4⁺ T-cells was successfully induced by both liposome formulations (Figure 5A & B), whereas few OT-II cells were present in mice that were vaccinated with peptide alone. Two different doses were used for vaccination. There were no differences in T-cell expansion in the high dose, but in the low dose treatment we observed increased expansion in the group which received the antigen with functionalized liposomes (Figure 5B).

The majority of the OT-II cells that were found in all organs were positive for the transcription factor T-bet. Few OT-II cells expressed Gata3, RORyt or FoxP3 (Supplementary figure 8), suggesting a Th1 profile. Indeed, upon *ex vivo* stimulation with PMA and ionomycin, IFN- γ was the most abundantly expressed cytokine (Figure 6A) while almost no IL-4 or IL-17 was expressed (Supplementary figure 9). We observed a significant increase in IFN- γ production after immunization with CPK-functionalized liposomes compared to non-functionalized liposomes. Interestingly, the expanded cells also produced IL-10 (Fig 6B) despite the absence of FoxP3 expression. The IL-10 production was significantly higher in mice that received functionalized liposomes. Further inspection of these cytokine-producing T-cells revealed an increase of double-producing OT-II cells after vaccination with functionalized liposomes (Figure 6C, D).

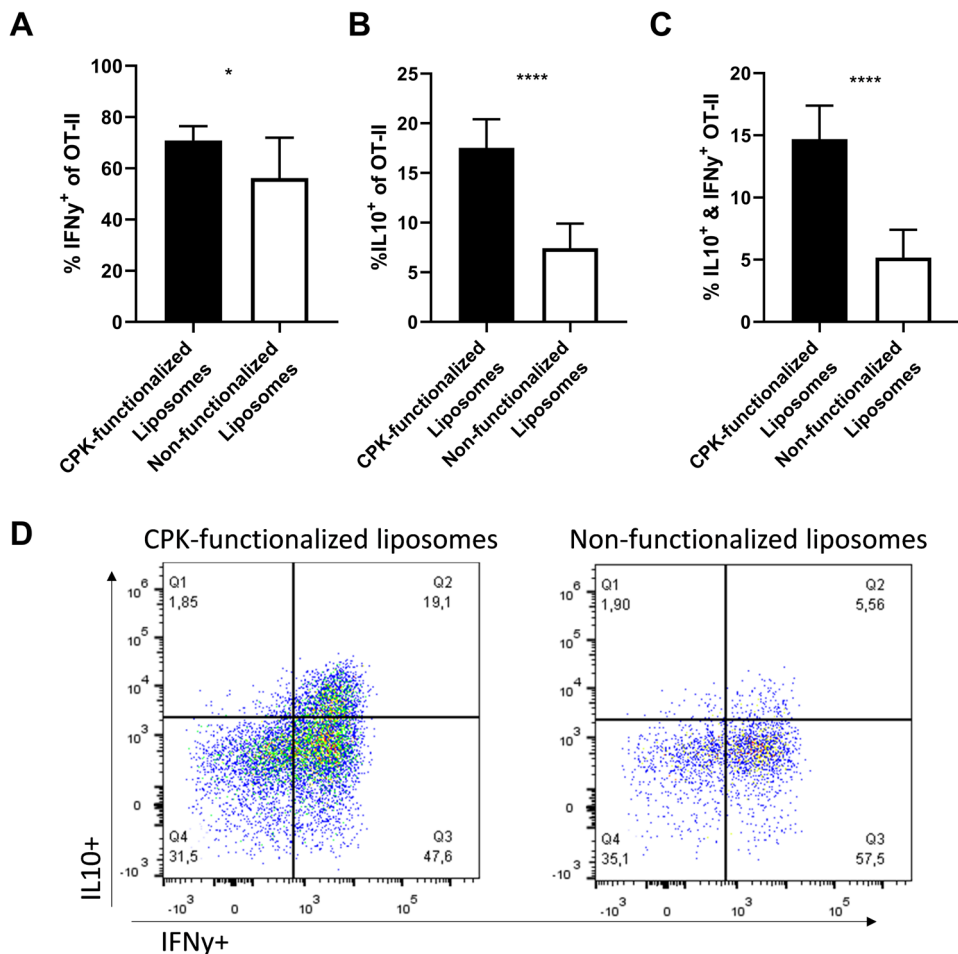


Figure 6. Cytokine production by expanded OT-II T-cells after ex vivo stimulation. OT-II cells that produced IFN- γ (A), IL-10 (B), and both IL-10 and IFN- γ (C) after stimulation for 6 hours with PMA and ionomycin from the spleen after vaccination with 1 nmol antigen associated with either CPK-functionalized or non-functionalized liposomes (mean \pm SD, $n \geq 6$). A representative FACS plot of OT-II cells for each formulation is shown in D. Mice where less than 200 OT-II cells were detected, were excluded from the analysis. Outliers were detected with Grubb's outliers test and groups were compared with an unpaired student's t test. * = $p < 0.05$, **** = $p < 0.0001$.

Discussion

In this study, we demonstrated a novel antigen association method to liposomes based on a complementary peptide pair that forms a CC upon interaction. PepK was coupled to cholesterol to yield CPK, which was encapsulated in the lipid bilayer, whereas pepE was synthesized with two different antigenic epitopes. The interaction between pepE and pepK was already known to be stable under physiological conditions [33, 44] and we now demonstrate its use as a method of antigen association. We established that incorporation of CPK in the liposomal

bilayers did not affect the size, polydispersity or zeta potential of liposomes composed of DSPC, DOTAP and cholesterol.

The binding affinity between pepK and pepE is in line with expected values reported before [45]. We observed Kds around 10^{-7} M when mixing both soluble peptides. This did not change when CPK-functionalized liposomes were used instead of soluble peptide or pepE-antigen was used instead of pepE. Moreover, we observed an increase in ellipticity in the CD spectrum, which strongly suggests that the association indeed occurs via the formation of a CC [36, 46]. By simple mixing of the antigen and liposomes, high efficiency adsorption was achieved. This adsorption is very stable and resulted in high co-localization of antigen and liposome both *in vitro* and *in vivo*.

We showed in both BMDCs and zebrafish embryos that peptides associated to non-functionalized liposomes, but not to functionalized liposomes, can rapidly dissociate from the liposomes. While we saw a degree of co-localization of antigen with non-functionalized liposomes, this was significantly increased when antigen was associated with functionalized liposomes. PepE-OVA323 was taken up by BMDCs and showed accumulation in zebrafish endothelial cells even without liposomes. This is constant with the net anionic charge of this peptide, which leads to rapid clearance by scavenger endothelial cells which are similar to liver sinusoidal endothelial cells in mammals [40]. CC association, as demonstrated, results in prolonged co-localization and therefore potentially increases exposure to antigen-coated liposomes and could result in more antigen presentation and TCR stimulation.

This prolonged TCR stimulation is in line with our *in vitro* observations, where we confirmed the adjuvant effect of cationic liposomes [1, 5]. Antigen association with non-functionalized liposomes resulted in a stronger T-cell proliferation, reducing the EC50 approximately 5-fold. Stronger antigen association to CPK-functionalized liposomes resulted in an 18-fold EC50 reduction compared to plain antigen in CD4⁺, but not in CD8⁺ T-cells. For CD8⁺ T-cells more proliferation was observed at higher pepE-OVA257 concentrations. The proliferation however was barely affected by the addition of either non-functionalized or functionalized liposomes to the formulation. This suggests that the T-cell proliferation is only induced by unbound antigen, but not liposome-associated antigen. Possibly the antigens associated to these liposomes are less capable of endosomal escape and therefore do not enter the cytosol after uptake by BMDCs. MHC-II restricted epitopes are loaded into MHC-II molecules in the late endosome, and therefore not affected by the absence of endosomal escape [47-50]. MHC-I restricted epitopes however require this escape to be efficiently cross-presented to MHC-I molecules in the ER [47, 50-52]. The potential lack of endosomal escape would be

surprising, as cationic liposomes are often used to induce CD8⁺ T-cell responses *in vitro* and *in vivo* [17-19], and are even found to promote cross presentation [22, 53, 54]. Apparently, this is not the case for the liposomes we have investigated. Strong T-cell expansion of transferred OT-II derived CD4⁺ T-cells was observed 1 week after vaccination with antigen associated to both non-functionalized and functionalized liposomes. When the vaccination was performed with 1 nmol of antigen, we found that approximately 5-6% of all CD4⁺ T-cells were expanded OT-II cells, which is in line with previous work [10]. Both liposomes directed the induced immune response towards a Th1 phenotype, as most of our OT-II cells expressed T-bet, which is in agreement with previous findings [9, 10, 21, 26]. Hardly any cells were expressing transcription factors associated with Th2 (Gata3), Th17 (RORγT) or Treg (FoxP3) phenotypes. This was confirmed by the cytokine production upon *ex vivo* stimulation of spleen-derived lymphocytes. Approximately 55% of all OT-II cells in the spleen were producing IFN-γ, a typical Th1 cytokine, in mice which received antigen associated with non-functionalized liposomes. In mice that received functionalized liposomes significantly more OT-II cells produced IFN-γ, suggesting a stronger immune response.

A striking difference was the production of IL-10 after immunization. In mice that received non-functionalized liposomes, approximately 7% of all OT-II cells produced IL-10, but in mice that were vaccinated with CPK-functionalized liposomes, over 15% produced IL-10. Practically all of these IL-10-producing cells were also producing IFN-γ. The double-producing CD4⁺ T-cells were previously observed in parasitic infections and have proven critical for host-survival. They are considered to dampen the ongoing immune response more effectively than ordinary regulatory T-cells [55-58]. They could be an interesting phenotype to induce in the treatment of auto-immune diseases and allergy, as both IFN-γ and IL-10 have an inhibitory effect on the Th2 immune response [56, 59, 60]. It is thought that this subset of IL-10- and IFN-γ-producing Th1 cells is the result of continuous antigen presentation and T-cell receptor (TCR) overstimulation [55, 58, 61-64]. This suggests that immunization with antigen associated to CPK-functionalized liposomes resulted in more stimulation of the TCRs by antigen presenting cells than antigen associated to non-functionalized liposomes, which could be explained by the enhanced affinity of pepE-OVA323 to functionalized liposomes.

In conclusion, we have demonstrated the use of CC-forming peptides as an antigen-attachment tool for peptide-based antigens. The antigens have a high affinity for the liposomes and have a high association efficiency. Moreover, the association remains intact *in vitro* and *in vivo* and could be used for peptide-based MHC-II restricted epitopes. The induced immune response by DCs pulsed with CC-adsorbed antigen to liposomes was much higher than for electrostatically

adsorbed antigen. Moreover, *in vivo* we observed a strong increase in IL-10- and IFN- γ -producing antigen-specific CD4⁺ T-cells, which suggests a stronger TCR stimulation after CC-mediated association of antigen.

Funding

This work was supported by the Nederlandse Organisatie voor Wetenschappelijk Onderzoek (TKI-NCI, grant 731.014.207).

Acknowledgements

We thank J. van Strien, A. Boyle, N. Crone, J. van Duijn, F. Lozano, S. Romeijn, K. Hajmohammadebrahimtehrani and A.I. Kotsogianni Teftsoglou for technical assistance.

Declaration of Interest

None.

References

1. Christensen, D., et al., *Cationic liposomes as vaccine adjuvants*. Expert Review of Vaccines, 2007. **6**(5): p. 785-796.
2. Varypatakis, E.M., et al., *Cationic liposomes loaded with a synthetic long peptide and poly(I:C): a defined adjuvanted vaccine for induction of antigen-specific T cell cytotoxicity*. The AAPS Journal, 2014. **17**(1): p. 216-226.
3. Schwendener, R.A., *Liposomes as vaccine delivery systems: a review of the recent advances*. Therapeutic Advances in Vaccines, 2014. **2**(6): p. 159-182.
4. Joshi, M.D., et al., *Targeting tumor antigens to dendritic cells using particulate carriers*. J Control Release, 2012. **161**(1): p. 25-37.
5. Benne, N., et al., *Orchestrating immune responses: How size, shape and rigidity affect the immunogenicity of particulate vaccines*. Journal of Controlled Release, 2016. **234**: p. 124-134.
6. Badiie, A., et al., *The role of liposome size on the type of immune response induced in BALB/c mice against leishmaniasis: rgp63 as a model antigen*. Experimental Parasitology, 2012. **132**(4): p. 403-409.
7. Watson, D.S., A.N. Endsley, and L. Huang, *Design considerations for liposomal vaccines: Influence of formulation parameters on antibody and cell-mediated immune responses to liposome associated antigens*. Vaccine, 2012. **30**(13): p. 2256-2272.
8. Bachmann, M.F. and G.T. Jennings, *Vaccine delivery: a matter of size, geometry, kinetics and molecular patterns*. Nature Reviews Immunology, 2010. **10**: p. 787-796.
9. Hussain, M.J., et al., *Th1 immune responses can be modulated by varying dimethyldioctadecylammonium and distearoyl-sn-glycero-3-phosphocholine content in liposomal adjuvants*. J Pharm Pharmacol, 2014. **66**(3): p. 358-66.
10. Benne, N., et al., *Anionic 1,2-distearoyl-sn-glycero-3-phosphoglycerol (DSPG) liposomes induce antigen-specific regulatory T cells and prevent atherosclerosis in mice*. J Control Release, 2018. **291**: p. 135-146.
11. Bal, S.M., et al., *Co-encapsulation of antigen and Toll-like receptor ligand in cationic liposomes affects the quality of the immune response in mice after intradermal vaccination*. Vaccine, 2011. **29**(5): p. 1045-1052.
12. Du, G., et al., *Immunogenicity of diphtheria toxoid and poly(I:C) loaded cationic liposomes after hollow microneedle-mediated intradermal injection in mice*. Int J Pharm, 2018. **547**(1-2): p. 250-257.
13. Henriksen-Lacey, M., et al., *Liposomal vaccine delivery systems*. Expert Opinion on Drug Delivery, 2011. **8**(4): p. 505-519.
14. Perrie, Y., et al., *A case-study investigating the physicochemical characteristics that dictate the function of a liposomal adjuvant*. Human Vaccines & Immunotherapeutics, 2013. **9**(6): p. 1374-1381.
15. Slütter, B., et al., *Antigen-Adjuvant Nanoconjugates for Nasal Vaccination: An Improvement over the Use of Nanoparticles?* Molecular Pharmaceutics, 2010. **7**(6): p. 2207-2215.
16. Slütter, B., et al., *Conjugation of ovalbumin to trimethyl chitosan improves immunogenicity of the antigen*. Journal of Controlled Release, 2010. **143**(2): p. 207-214.
17. Varypatakis, E.M., et al., *Cationic Liposomes Loaded with a Synthetic Long Peptide and Poly(I:C): a Defined Adjuvanted Vaccine for Induction of Antigen-Specific T Cell Cytotoxicity*. The AAPS Journal, 2015. **17**(1): p. 216-226.

18. Varypataki, E.M., et al., *Cationic DOTAP-based liposomes: a vaccine formulation platform for synthetic long peptides with widely different physicochemical properties*, in *Leiden Academic Center for Drug Research*. 2016, Leiden University: Leiden.
19. Heuts, J., et al., *Cationic Liposomes: A Flexible Vaccine Delivery System for Physicochemically Diverse Antigenic Peptides*. *Pharmaceutical Research*, 2018. **35**(11).
20. Colletier, J.-P., et al., *Protein encapsulation in liposomes: efficiency depends on interactions between protein and phospholipid bilayer*. *BMC Biotechnology*, 2002. **2**(1): p. 2-9.
21. Henriksen-Lacey, M., et al., *Liposomes based on dimethyldioctadecylammonium promote a depot effect and enhance immunogenicity of soluble antigen*. *J Control Release*, 2010. **142**(2): p. 180-186.
22. Schmidt, S.T., et al., *The administration route is decisive for the ability of the vaccine adjuvant CAF09 to induce antigen-specific CD8+ T-cell responses: The immunological consequences of the biodistribution profile*. *Journal of Controlled Release*, 2016. **239**: p. 107-117.
23. Kaur, R., et al., *Effect of Incorporating Cholesterol into DDA:TDB Liposomal Adjuvants on Bilayer Properties, Biodistribution, and Immune Responses*. *Molecular Pharmaceutics*, 2014. **11**(1): p. 197-207.
24. Henriksen-Lacey, M., et al., *Comparison of the Depot Effect and Immunogenicity of Liposomes Based on Dimethyldioctadecylammonium (DDA), 3β-[N-(N',N'-Dimethylaminoethane)carbonyl] Cholesterol (DC-Chol), and 1,2-Dioleoyl-3-trimethylammonium Propane (DOTAP): Prolonged Liposome Retention Mediates Stronger Th1 Responses*. *Molecular Pharmaceutics*, 2011. **8**(1): p. 153-161.
25. Henriksen-Lacey, M., et al., *Liposomal cationic charge and antigen adsorption are important properties for the efficient deposition of antigen at the injection site and ability of the vaccine to induce a CMI response*. *J Control Release*, 2010. **145**(2): p. 102-108.
26. Hamborg, M., et al., *Elucidating the mechanisms of protein antigen adsorption to the CAF/NAF liposomal vaccine adjuvant systems: Effect of charge, fluidity and antigen-to-lipid ratio*. *Biochimica et Biophysica Acta (BBA) - Biomembranes*, 2014. **1838**(8): p. 2001-2010.
27. Robson Marsden, H. and A. Kros, *Self-assembly of coiled coils in synthetic biology: inspiration and progress*. *Angew Chem Int Ed Engl*, 2010. **49**(17): p. 2988-3005.
28. Versluis, F., H.R. Marsden, and A. Kros, *Power struggles in peptide-amphiphile nanostructures*. *Chemical Society Reviews*, 2010. **39**(9): p. 3434-3444.
29. Beesley, J.L. and D.N. Woolfson, *The de novo design of α-helical peptides for supramolecular self-assembly*. *Current Opinion in Biotechnology*, 2019. **58**: p. 175-182.
30. Kong, L., et al., *Light-Triggered Cancer Cell Specific Targeting and Liposomal Drug Delivery in a Zebrafish Xenograft Model*. *Advanced Healthcare Materials*, 2020. **9**(6): p. 1901489.
31. Kong, L., et al., *Temporal Control of Membrane Fusion through Photolabile PEGylation of Liposome Membranes*. *Angewandte Chemie International Edition*, 2016. **55**(4): p. 1396-1400.
32. Yang, J., et al., *Application of Coiled Coil Peptides in Liposomal Anticancer Drug Delivery Using a Zebrafish Xenograft Model*. *ACS Nano*, 2016. **10**(8): p. 7428-35.

33. Oude Blenke, E.E., et al., *Coiled coil interactions for the targeting of liposomes for nucleic acid delivery*. *Nanoscale*, 2016. **8**(16): p. 8955-8965.
34. Yang, J., et al., *Drug Delivery via Cell Membrane Fusion Using Lipopeptide Modified Liposomes*. *ACS Central Science*, 2016. **2**(9): p. 621-630.
35. Versluis, F., et al., *In Situ Modification of Plain Liposomes with Lipidated Coiled Coil Forming Peptides Induces Membrane Fusion*. *Journal of the American Chemical Society*, 2013. **135**(21): p. 8057-8062.
36. Crone, S.N., et al., *Peptide-Mediated Liposome Fusion: The Effect of Anchor Positioning*. *International Journal of Molecular Sciences*, 2018. **19**(1).
37. Wang, W., et al., *Culture and Identification of Mouse Bone Marrow-Derived Dendritic Cells and Their Capability to Induce T Lymphocyte Proliferation*. *Medical science monitor : international medical journal of experimental and clinical research*, 2016. **22**: p. 244-250.
38. Miltenyi, *CD4+ T Cell Isolation Kit_mouse_#130-104-454*. 2016.
39. Hogan, B.M., et al., *cceb1 is required for embryonic lymphangiogenesis and venous sprouting*. *Nature Genetics*, 2009. **41**: p. 396-398.
40. Campbell, F., et al., *Directing Nanoparticle Biodistribution through Evasion and Exploitation of Stab2-Dependent Nanoparticle Uptake*. *ACS Nano*, 2018. **12**(3): p. 2138-2150.
41. Schindelin, J., et al., *Fiji: an open-source platform for biological-image analysis*. *Nature Methods*, 2012. **9**: p. 676-682.
42. Schneider, C.A., W.S. Rasband, and K.W. Eliceiri, *NIH Image to ImageJ: 25 years of image analysis*. *Nature Methods*, 2012. **9**: p. 671-675.
43. Ollion, J., et al., *TANGO: a generic tool for high-throughput 3D image analysis for studying nuclear organization*. *Bioinformatics*, 2013. **29**(14): p. 1840-1841.
44. Poulcharidis, D., et al., *A flow cytometry assay to quantify intercellular exchange of membrane components*. *Chemical Science*, 2017. **8**(8): p. 5585-5590.
45. Litowski, J.R. and R.S. Hodges, *Designing Heterodimeric Two-stranded α -Helical Coiled-coils: effects of hydrophobicity and α -helical propensity on protein folding, stability and specificity* *Journal of Biological Chemistry*, 2002. **277**(40): p. 37272-37279.
46. Rabe, M., H.R. Zope, and A. Kros, *Interplay between Lipid Interaction and Homocooling of Membrane-Tethered Coiled-Coil Peptides*. *Langmuir*, 2015. **31**(36): p. 9953-9964.
47. Neefjes, J., et al., *Towards a systems understanding of MHC class I and MHC class II antigen presentation*. *Nature Reviews Immunology*, 2011. **11**: p. 823-836.
48. van den Hoorn, T., et al., *Routes to manipulate MHC class II antigen presentation*. *Current Opinion in Immunology*, 2011. **23**(1): p. 88-95.
49. Delamarre, L., H. Holcombe, and I. Mellman, *Presentation of Exogenous Antigens on Major Histocompatibility Complex (MHC) Class I and MHC Class II Molecules Is Differentially Regulated during Dendritic Cell Maturation*. *The Journal of Experimental Medicine*, 2003. **198**(1): p. 111-122.
50. Guermonprez, P., et al., *Antigen Presentation and T Cell Stimulation by Dendritic Cells*. *Annual Review of Immunology*, 2002. **20**(1): p. 621-667.
51. Banchereau, J. and R.M. Steinman, *Dendritic cells and the control of immunity*. *Nature*, 1998. **392**: p. 245-252.
52. Burgdorf, S., et al., *Distinct Pathways of Antigen Uptake and Intracellular Routing in CD4 and CD8 T Cell Activation*. *Science*, 2007. **316**(5824): p. 612-616.

53. Gao, J., et al., *Cationic liposomes promote antigen cross-presentation in dendritic cells by alkalizing the lysosomal pH and limiting the degradation of antigens*. International journal of nanomedicine, 2017. **12**: p. 1251-1264.
54. Joffre, O.P., et al., *Cross-presentation by dendritic cells*. Nature Reviews Immunology, 2012. **12**: p. 557-569.
55. Villegas-Mendez, A., et al., *Parasite-Specific CD4+ IFN-gamma+ IL-10+ T Cells Distribute within Both Lymphoid and Nonlymphoid Compartments and Are Controlled Systemically by Interleukin-27 and ICOS during Blood-Stage Malaria Infection*. Infect Immun, 2016. **84**(1): p. 34-46.
56. Ng, T.H., et al., *Regulation of adaptive immunity; the role of interleukin-10*. Front Immunol, 2013. **4**.
57. Sun, J., et al., *Effector T cells control lung inflammation during acute influenza virus infection by producing IL-10*. Nat Med, 2009. **15**(3): p. 277-84.
58. Jankovic, D., et al., *Conventional T-bet(+)Foxp3(-) Th1 cells are the major source of host-protective regulatory IL-10 during intracellular protozoan infection*. J Exp Med, 2007. **204**(2): p. 273-283.
59. Akdis, M. and C.A. Akdis, *Mechanisms of allergen-specific immunotherapy*. Journal of Allergy and Clinical Immunology, 2007. **119**(4): p. 780-789.
60. Larche, M., C.A. Akdis, and R. Valenta, *Immunological mechanisms of allergen-specific immunotherapy*. Nat Rev Immunol, 2006. **6**(10): p. 761-771.
61. Gabrysova, L., et al., *c-Maf controls immune responses by regulating disease-specific gene networks and repressing IL-2 in CD4(+) T cells*. Nat Immunol, 2018. **19**(5): p. 497-507.
62. Villegas-Mendez, A., et al., *Long-Lived CD4+IFN-gamma+ T Cells rather than Short-Lived CD4+IFN-gamma+IL-10+ T Cells Initiate Rapid IL-10 Production To Suppress Anamnestic T Cell Responses during Secondary Malaria Infection*. J Immunol, 2016. **197**(8): p. 3152-3164.
63. Jankovic, D., D.G. Kugler, and A. Sher, *IL-10 production by CD4+ effector T cells: a mechanism for self-regulation*. Mucosal Immunol, 2010. **3**(3): p. 239-246.
64. O'Garra, A. and P. Vieira, *TH1 cells control themselves by producing interleukin-10*. Nature Reviews Immunology, 2007. **7**(6): p. 425-428.

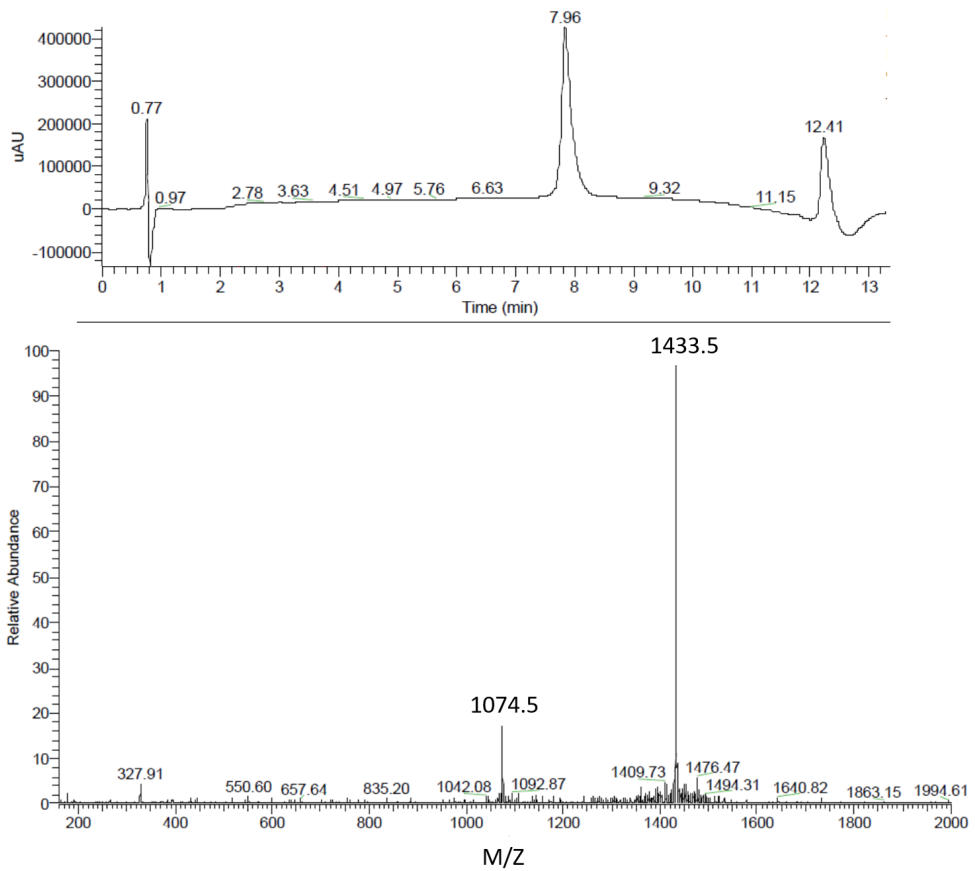
Supplements

Supplementary table 1 Overview of all fluorescent antibodies used for flow cytometry. All antibodies were purchased from eBioscience.

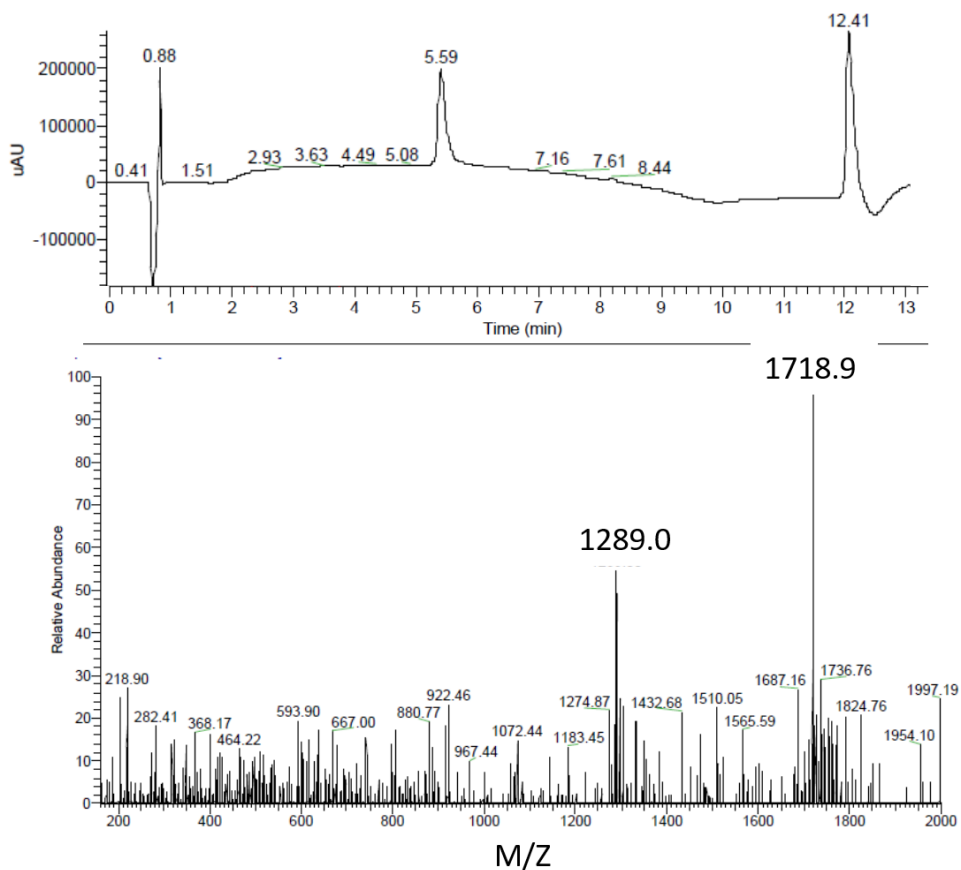
Antibody Target	Fluorescent label
CD25	PE
CD4	APC
CD4	PE
CD4	V500
CD45.1	eFluor 450
CD8	eFluor 450
Fixable Viability Dye	eFluor 780
FOXP3	APC
FOXP3	eFluor 450
Gata3	PE
IFN- γ	BV650
IL-10	PE
IL-17	FITC
IL-4	APC
Ki-67	FITC
ROR γ T	BV650
T-bet	PE-cy7
Thy1.2	PE
Thy1.2	PE-cy7
Thy1.2	PerCP

Supplementary table 2. Overview of all peptides that were synthesized. All names that are used throughout the manuscript with the sequence, calculated theoretical molecular weight (MW) and expected mass per charge (m/z) values for different positive charges (2, 3 and 4 protons added) which will be measured in mass spectrometry.

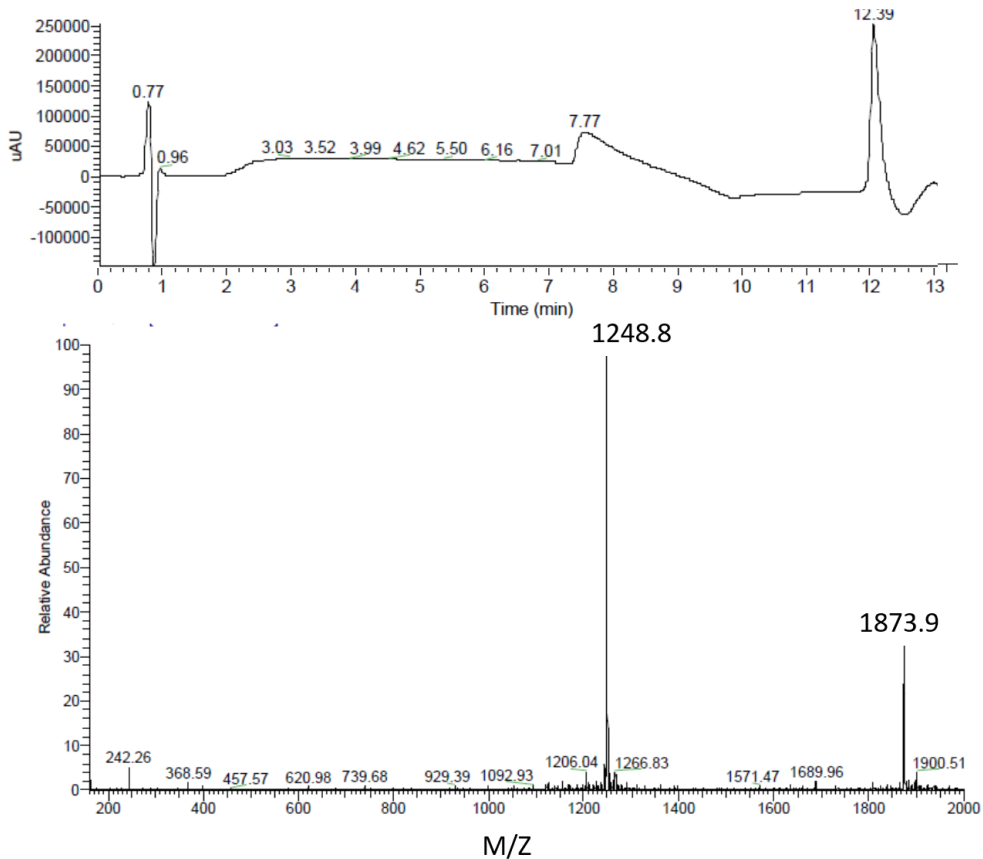
Name	Sequence	MW (Da)	2+ m/z	3+ m/z	4+ m/z
CPK	cholesterol – (PEG)4 – KIAALKEKIAALKEKIAALKEKIAALKE	3747.2	1874.6	1250.1	937.8
pepE-OVA323	YGEIAALEKEIAALEKEIAALEKISQAVHAAHAEINEAGR	4299.3	2150.7	1434.1	1075.8
pepE-OVA257	YGEIAALEKEIAALEKEIAALEKSIINFEKL	3489.0	1745.5	1164.0	873.3
pepE-OVA323-AF488	GC-AF488	5160.9	2581.5	1721.3	1291.2



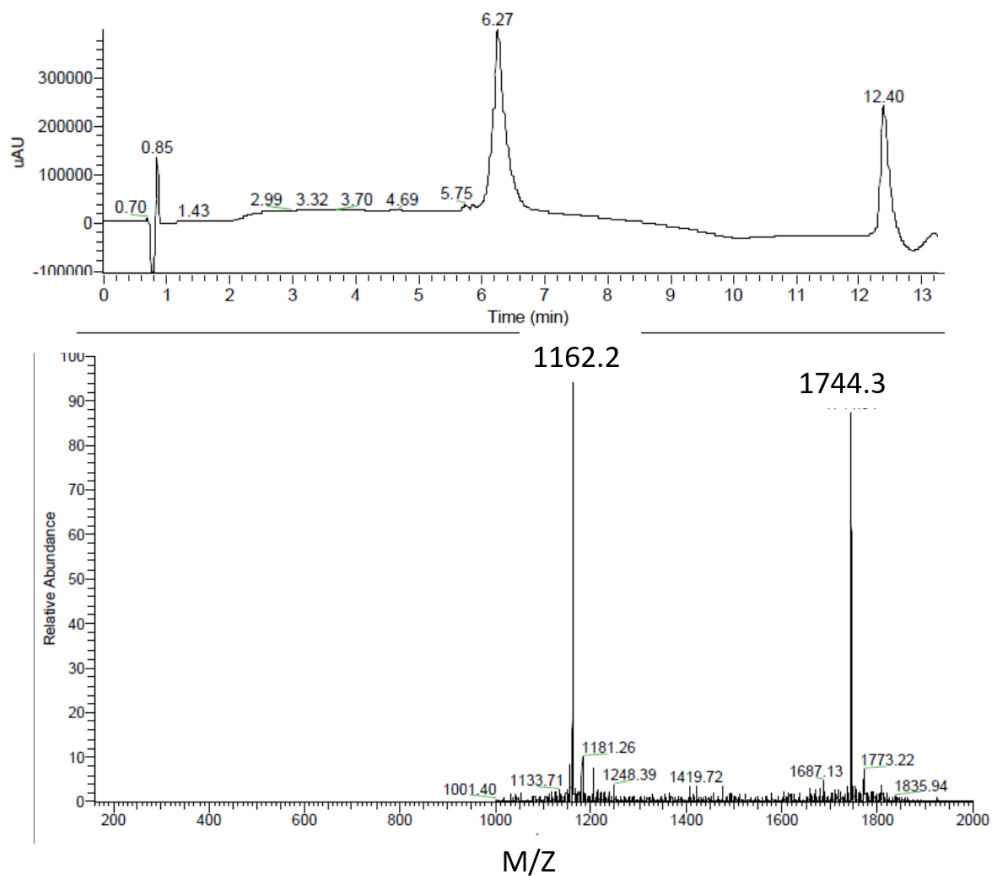
Supplementary Figure 1. LC (top) chromatogram and MS (bottom) spectrum of LC peak at 7.96 minute of pepE-OVA323. The sequence of acetylated pepE-OVA323 is Ac-YGEIAALEKEIAALEKEIAA LEKISQAVHAAHAEINEAGR, which has a molecular mass of 4299.3. the expected m/z values are: 1434.1 and 1075.8 for 3+ and 4+, respectively.



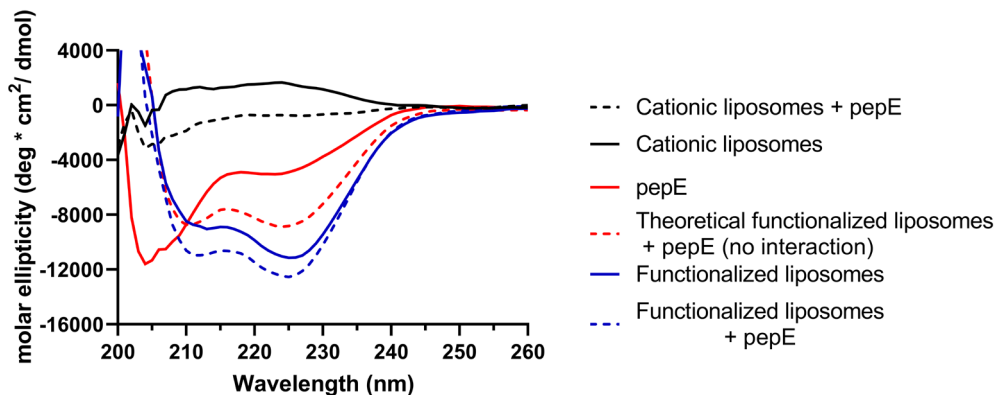
Supplementary Figure 2. LC (top) chromatogram and MS (bottom) spectrum of peak at 5.59 min of acetylated pepE-OVA323-AF488. The sequence of pepE-OVA323-AF488 is Ac-YGEIAALEKEIAALEKEIAALEKISQAVHAAHAEINEAGRGC-AF488, which has a molecular mass of 5160.9. the expected m/z values are: 1721.3 and 1291.2 for 3+ and 4+, respectively.



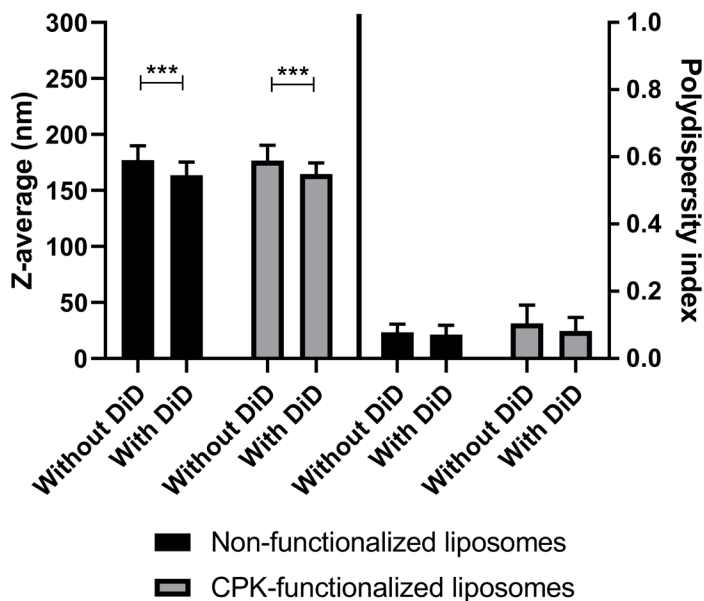
Supplementary Figure 3. LC (top) chromatogram and MS (bottom) spectrum of peak at 7.77 minute of CPK. The sequence of CPK is cholesterol-PEG4-KIAALKEKIAALKEKIAALKEKIAALKE, which has a molecular mass of 3747.2. The expected m/z values are: 1874.6 and 1250.1 for 2+ and 3+, respectively.



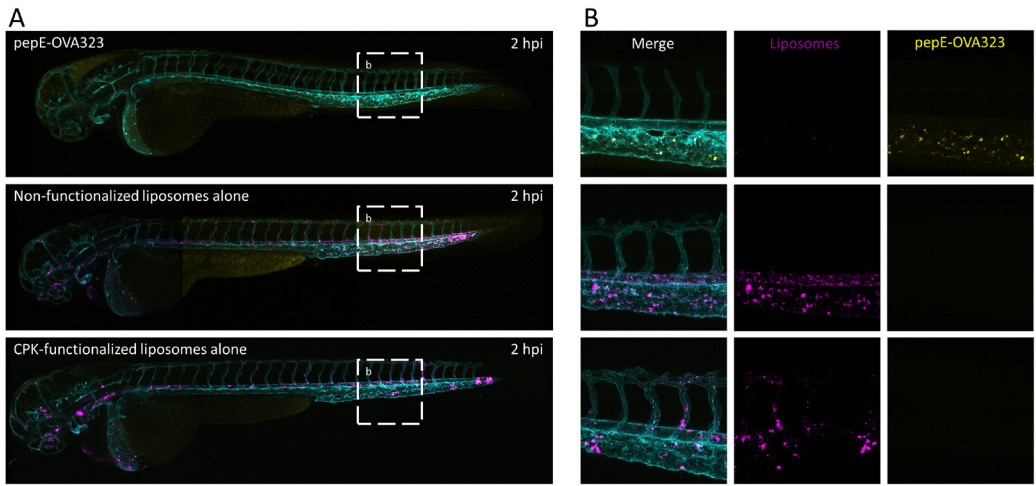
Supplementary Figure 4. LC (top) chromatogram and MS (bottom) spectrum of peak at 6.27 min of acetylated pepE-OVA257. The sequence of pepE-OVA257 is Ac-YGEIAALEKEIAALEKEIAALEKSIIN FEKL, which has a molecular mass of 3489.0. the expected m/z values are: 1745.5 and 1164.0 for 2+ and 3+, respectively.



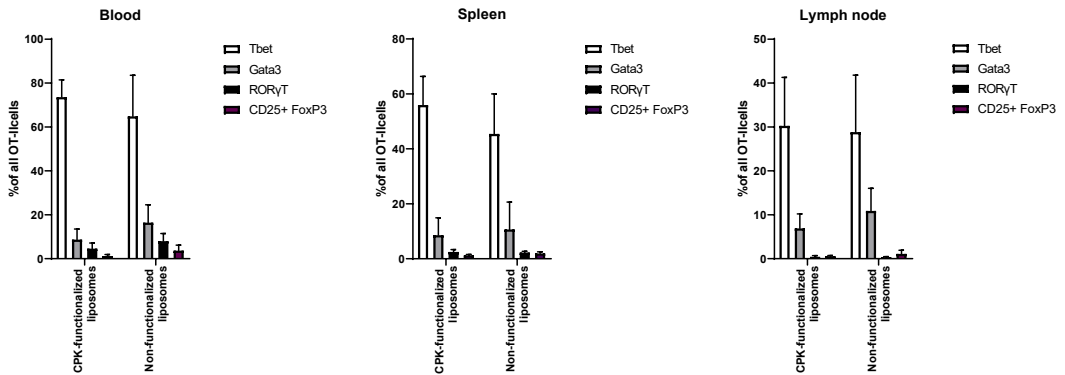
Supplementary Figure 5. Far-UV circular dichroism spectrum of pepE and liposomes with and without CPK. Plain (black) and functionalized liposomes (blue) with (dashed lines) and without pepE (connected lines). The spectrum of pepE (red, connected line) and the theoretical spectrum of pepE and functionalized liposomes if there is no interaction (red, dashed). Non-functionalized liposomes, for calculation purpose, were considered to have the same molar amount of CPK as functionalized liposomes. All lines were smoothed (7 neighbors).



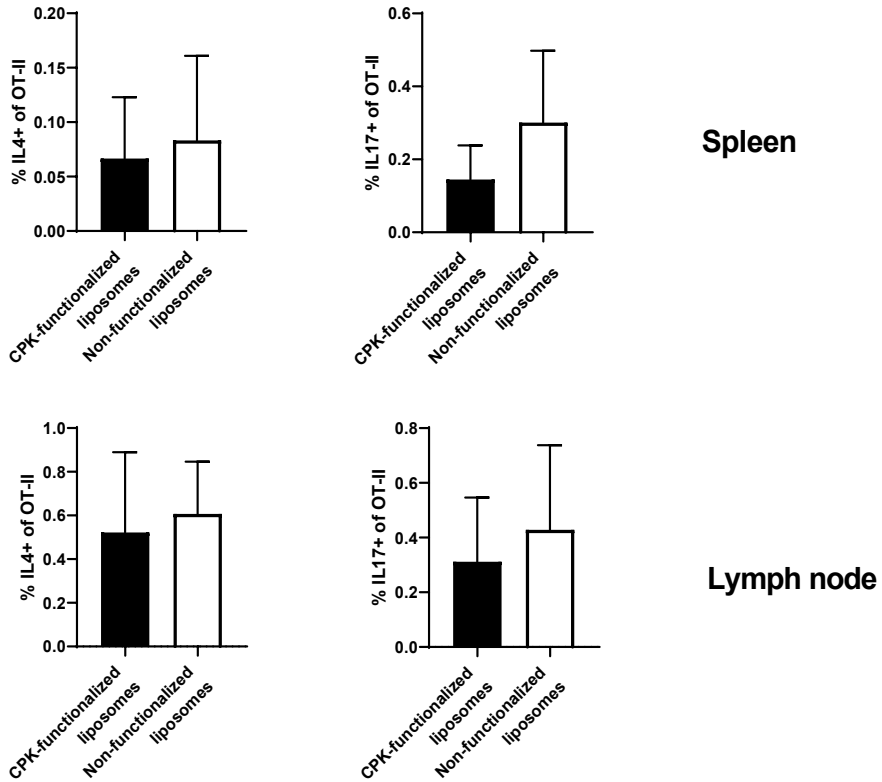
Supplementary Figure 6. Effect of fluorophore DiD on liposome size and polydispersity index. Measured hydrodynamic diameter (Z-average) of liposomes with or without fluorophore (mean \pm SD, $n \geq 9$, of at least 3 separate formulations). Groups were compared in a two-way ANOVA with a Sidak's multiple comparison post-test. ** = $p < 0.01$



Supplementary Figure 7. Distribution of pepE-OVA323, non-functionalized liposomes and CPK-functionalized liposomes in zebrafish embryo 2 hour post injection. Gray arrows indicate the injection site. The vasculature (cyan), peptide (yellow) and liposomes (magenta) were visualized in a confocal microscope at 10x magnification (A) and 40x magnification (B).



Supplementary Figure 8. Percentage of cell that expressed Tbet, Gata3, RORγT or CD25 and Foxp3 of OT-II cells measured by flow cytometry found in blood, spleen and lymph node after vaccination with 1 nmol antigen with either non-functionalized or CPK-functionalized liposomes (mean \pm SD, n = 8). Only mice where more than 100 OT-II cells were found, were considered for this analysis, so negative controls are not shown.



Supplementary Figure 9. Ex vivo cytokine production. Lymphocytes of mice vaccinated with pepE-OVA323 and non-functionalized or CPK-functionalized liposomes were stimulated for 6 hour with PMA and ionomycin of which 5 with Brefeldin A. The percentage of OT-II cells that produced IL-4 and IL-17 was measured by flow cytometry (mean \pm SD).



<https://youtu.be/EEJNRSuJ1PY>

Supplementary video 1. 3D projection of zebrafish embryo tail vasculature (cyan) 2 hours after injection of cationic liposomes (magenta) with pepE-OVA323 (yellow).



<https://youtu.be/rki5ATyZgOM>

Supplementary video 2. 3D projection of zebrafish embryo tail vasculature (cyan) 2 hours after injection of functionalized liposomes (magenta) with pepE-OVA323 (yellow).

